Magnetism induced by excess electrons trapped at diamagnetic edge-quantum well in multi-layer graphene

Xi Zhang, Chao Wang, Chang Q Sun, and Dongfeng Diao

Citation: Applied Physics Letters **105**, 042402 (2014); doi: 10.1063/1.4891558
View online: http://dx.doi.org/10.1063/1.4891558
View Table of Contents: http://scitation.aip.org/content/aip/journal/apl/105/4?ver=pdfcov
Published by the AIP Publishing

Magnetism induced by excess electrons trapped at diamagnetic edge-quantum well in multi-layer graphene

Xi Zhang,[1,2] Chao Wang,[1] Chang Q Sun,[2] and Dongfeng Diao[1,a)]
[1]*Institute of Nanosurface Science and Engineering, Shenzhen University, Shenzhen 518060, China*
[2]*NOVITAS, School of Electrical and Electronic Engineering, Nanyang Technological University, Singapore 639798*

(Received 12 June 2014; accepted 17 July 2014; published online 28 July 2014)

In this paper, we clarified a robust mechanism of magnetism generated by excess electrons captured by edge-quantum well of diamagnetic armchair edges. Consistency between density functional theory calculations and electron cyclotron resonance experiments verified that: (1) Multi-layer armchair nanoribbons are stable with proper amounts of excess electrons which can provide net spin; (2) Since under-coordination induces lattice relaxation and potential well modulation, electrons tend to be trapped at edges; and (3) Neither large amount of excess electrons nor positive charges can induce magnetism. This work shed light on the development of graphene devices in its magnetic applications. © *2014 AIP Publishing LLC*.
[http://dx.doi.org/10.1063/1.4891558]

The physical origin of magnetism in graphene is a crucial issue for understanding its unique properties such as massless Dirac Fermions,[1,2] half-metallic conductivity,[3,4] quantum spin hall effect,[5,6] and its potential applications in spintronic devices.[7] However, the mechanism of graphene magnetism is complicated and inconclusive yet. The presence of local magnetism of graphene is edge-selected. The occurrence of anti-ferromagnetism at a zigzag edge was reported by 1.28 μ_{Bohr} (Bohr magnetron) in value in density functional theory (DFT) calculation[8] and the localized mid-gap state was identified by experiment at an atomic vacancy on graphite surface;[9] while the local magnetism can hardly be observed at either a clean graphite surface or an armchair edge. The edge-selectivity of the magnetism for π electrons can be understood from the angle of broken symmetry of the pseudo spin in different edges,[10] and also from Clar's aromatic sextet rule in chemistry with the different aromatic stabilities.[11,12] Recent theoretical work based on edge-corrected mean-field Hubbard model[13] explained the origin of the weak magnetic moment of π electrons at edge from the perspective of edge lattice relaxation and potential well deepening induced by under-coordination effect. It is also clarified that the dangling σ-bond with a dominant spin moment can be easily annihilated by the edge C-C bond reconstruction along certain kinds of edges, leading to the edge-selectivity of its magnetism.[13]

Due to the instability of dangling σ-bond, the experimental detection of magnetism of graphene becomes a challenging task.[14] Moreover, the anti-ferromagnetism of zigzag edge is also hardly identified because zigzag edges are thermodynamically unstable due to its less aromaticity.[11,12] The Scanning Tunneling Microscopy (STM) results prove that zigzag edges are much less frequently observed than armchair edges,[15] agreeing with calculated results.[16,17] Thus, although theoretical calculations show a considerable magnetism of graphene, experimental observations of mass magnetization M were always small (typically, less than ~0.1 emu/g), regardless of its forms such as highly oriented pyrolytic graphite, nanographites, nanodiamonds or disordered carbon films.[14]

Recently, a low-energy irradiation technique was developed in electron cyclotron resonance (ECR) plasma to synthesize multilayer graphene nanoflakes on carbon films and magnetism of the multilayer graphene nanoflakes was observed.[18] Our latest experimental results (as shown in Figure 1 with experimental method available in supplementary material[19]) observed a considerable large magnetization (~0.37 emu/g) above room temperature (300 K) of the multilayer graphene nanoflakes grown by electron irradiation assisting deposition. It was challenging to understand such a high magnetism.

Atomic under-coordination occurs at defects and edges of graphene and induces edge C-C bond contraction.[20] As a result, a deepened quantum well forms at the edge of graphene.[21] In the growing process of electron irradiation method, excess electrons may exist in the graphene, similar to electron n-type doping in the epitaxial graphene.[22] Thus, it can be expected that the edge-quantum well of graphene can trap the excess electron from e-beam and also its spin at

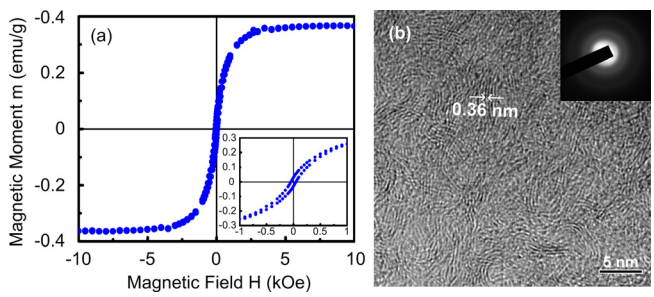

FIG. 1. (a) Unit magnetic moment (emu/g) of graphene nanoflake-contained carbon film. Inset graph shows a smaller field region of the hysteresis loop. (b) Plan-view transmission electron microscopy image of the carbon film. Inset is the electron diffraction pattern.

a)Author to whom correspondence should be addressed. Electronic mail: dfdiao@szu.edu.cn

edge sites. In this Letter, using dispersion-corrected DFT calculations, we will investigate the stability, distribution and spin of excess charges in the multi-layer armchair graphene nanoribbon (AGNR), which can be easily observed by experiments but was considered diamagnetic, to clarify the mechanism of the excess magnetism.

Figure 2 illustrates the principle of the magnetism of excess electron trapped by edge-quantum well. Generally, materials at the nano scale can be represented by a high fraction of atoms with an effective atomic coordination number.[21,23] Under-coordination will induce the bond relaxation at the local sites. Due to under-coordination, the C-C bond length (d_1) at edge will contract significantly compared with that of center (d_0) to lower the total energy. Meanwhile, the C-C bond lengths around the edge site (d_2) will show fluctuations and even expand to some extent. The bond contractions were reported to happen globally to dimers,[24] nanotubes,[25] atomic vacancies,[26] and so on. The contraction of edge C-C bond and the fluctuations of bond lengths along the finite carbon chain were also obtained by DFT calculation.[27] The shorter bonds between under-coordinated atoms will spontaneously accompany with the increase of bond energy. The potential well to the neighbor electrons will be deepened at the edge site with a consequence of localized densification of charge, energy and mass.[21] In the growing process under ECR plasma, excess electrons tend to be captured by the edge-quantum well of graphene. Meanwhile, they also have a small chance to be attracted among the inside potential wells. Locally trapped excess electrons can provide unpaired spin and induce relatively large magnetic moment at edge sites. In contrast, excess positive charges are not able to stay stably in the edge-quantum well due to the repulsion force from the C atomic ions.

DFT calculations were performed using the Dmol[3] code.[28] Up to three-layer AGNR (periodic in x direction) was modeled with a 1-nm vacuum slab in both the y (ribbon width) and the z (layer stacking) directions. All the AGNRs are modeled of 20-atom width, containing 40, 80, and 120 atoms per unit cell for monolayer, bilayer, and trilayer AGNR, respectively. The Perdew–Burke–Ernzerhof (PBE) functional[29] in the generalized gradient approximation is chosen to describe the exchange-correlation energy. The Tkatchenko-Scheffler scheme[30] of dispersion-correction is used to describe the vdW interactions. The all-electron method was used to describe the wave functions with a double numeric and polarization basis sets. Spin-unrestricted calculations were performed with both formal spin and manually set spin as initials. The results reported are corresponding to the spin configuration with the lowest total energy. Thermal smearing of 0.005 Ha was first used in the initial geometry optimizations of trilayer AGNRs. The smearing was removed in all the final energy calculations. In Dmol[3] code, the amount of excess charges, e(excess), was specified at the beginning of calculations. The amount of signed charges represents the total number of excess charge per unit cell. The active electrons of all the atoms plus the signed excess charges of the unit cell is the total active electrons considered in electronic structure calculations. The total energy, electronic structure, and electron densities are solved by self-consistent field (SCF) method towards the minimum of total energy. The self-consistency threshold of total energy was set at 10^{-6} Hartree. The geometry optimization was performed to obtain the optimized structure, electronic structure, and electron densities towards the global minimum of total energy and converged with the tolerances for the energy, force and displacement at 10^{-5} Hartree, 0.002 Hartree/Å, and 0.005 Å, respectively.

Figure 3 shows the total energy (E_{total}, eV) and total spin (μ_{Bohr}) per unit cell of monolayer, bilayer, and trilayer AGNRs as the e(excess) changes from 2 to −5. The E_{total} of e(excess) = 0 is taken as reference for each thickness. As shown in Figure 3(a), positive E_{total} for positive excess charges indicate that all the three thicknesses of AGNRs are

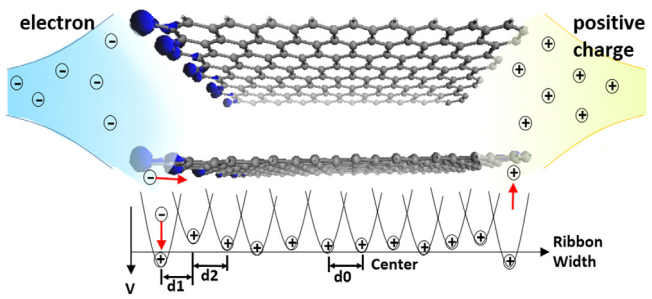

FIG. 2. Illustration of the magnetism of excess electron trapped by edge-quantum well. The changes of bond length at edge (d_1) and surrounding edge (d_2) compared with that of center (d_0) and bond energies will modulate the crystal potential well to electrons. Red arrows indicate the excess electrons will be likely trapped at edge and provide unpaired spin (blue isosurface), or in a small chance attracted among the inside potential wells; while excess positive charges will be repulsed and become unstable.

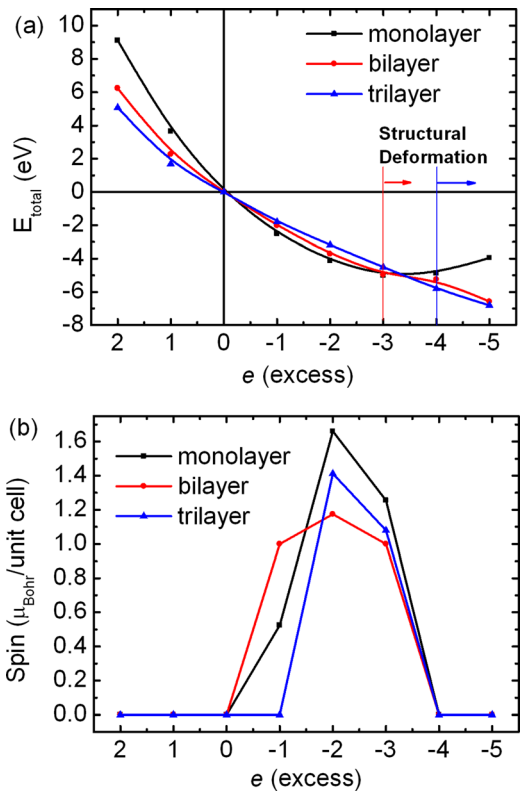

FIG. 3. (a) Total energy (eV) and (b) total spin (μ_{Bohr}) per unit cell of monolayer, bilayer, and trilayer AGNR versus excess charges ranging from 2 to −5. The total energy of e(excess) = 0 is set as reference for each thickness.

difficult to absorb positive charges. In contrast, the increasing negative e(excess) decreases the E_{total} and makes the structures more stable. However, too large amount of electrons slightly increase the E_{total} of monolayer AGNR ($e < -3$) instead. The increment of exchange-correlation energy of multi-electron interactions should take responsibility of the increase of E_{total}. Too large amount of electrons also induce structural deformation of bilayer ($e < -3$) and trilayer ($e < -4$) AGNRs (see Figure 4(a) and Figure S3 (Ref. 19)). The repulsive force among excess electrons in different layers results in the separation of bilayer and trilayer AGNR.

Figure 3(b) shows that high spin moments of 1.66, 1.17, and 1.41 μ_{Bohr} are obtained at e(excess) $= -2$ per unit cell for monolayer, bilayer, and trilayer AGNR, respectively. Fractional spin moments are obtained because the AGNR structure is a periodic system and the wave functions in the form of Bloch sums are delocalized. Results in Figure 3(b) indicate that only proper amount of excess electrons can induce spin moment for originally diamagnetic AGNR. But for too large amounts of excess electrons or positive charges, there are no net spin observed. The reason lies in the fact that the exchange energy lowered by parallel spin electrons cannot compensate the increment of the total energy caused by parallel occupation of higher energy states.

Moreover, since the total number of carbon atoms is proportional to the thickness of AGNR in a unit cell, the total spin per atom is actually largest in monolayer AGNR. Since $1\mu_{Bohr} = 9.274 \times 10^{-21}$ emu, considering only spin magnetic moment of AGNR as obtained in Figure 3(b), the mass magnetizations (M) are hence obtained as 19.25 emu/g, 6.78 emu/g, and 5.45 emu/g for monolayer, bilayer, and trilayer AGNR at the e(excess) $= -2$ for largest spins. The large M (19.25 emu/g) for charged infinite monolayer AGNR, although less than ~90 emu/g of bulk Fe_3O_4, is comparable to ~20 emu/g of bulk Fe_7S_8. Results indicate that monolayer AGNR has the best trapping ability among the three thicknesses. The reason is that monolayer graphene has the least coordination number, even in the interior of the ribbon.

Figure 4 shows the localized spin moment in bilayer and trilayer AGNR and the structural distortion caused by excess electrons in bilayer AGNR. The spin density distributions in Figure 4 indicate that the net spin densities are indeed localized at edge sites, verifying our principle of the edge-quantum well. The similar spin distributions are also shown in Figures S1 and S2 (Ref. 19) for monolayer and bilayer AGNR.

Figure 4(a) also indicates the structural distortion of bilayer AGNR caused by large amount of excess electrons (e $= -3$), mainly in the separation between layers around edge sites. Large amount of excess electrons (e $= -4$) also induces structural distortion of trilayer AGNR, as shown in Figure S3.[19] Two outside layers of trilayer AGNR are pushed away from the inside layer and bent outward. The repulsive force among excess electrons increases the inter-layer distance from ~3.8 Å to ~4.2 Å in center and further to ~5.0 Å at edge and also induce the inter-layer lattice mismatch of trilayer AGNR.

Figure 5(a) shows the profiles of Mulliken charge and spin along the ribbon width direction in trilayer AGNR unit cell at e(excess) $= -2$. The Mulliken charge and spin distributions are symmetric for both sides from the center along the width direction. Also, populations in two outside layers of trilayer AGNR are symmetric. The outmost and second outmost edge sites are labeled as C1 and C2, respectively. The bond lengths at C1 site decrease to 0.1254 nm (by −11.7%) in outside layer compared with the bulk value 0.1420 nm. The contraction of edge C-C bond deepens the edge potential well and induces fluctuation to the C2 sites.

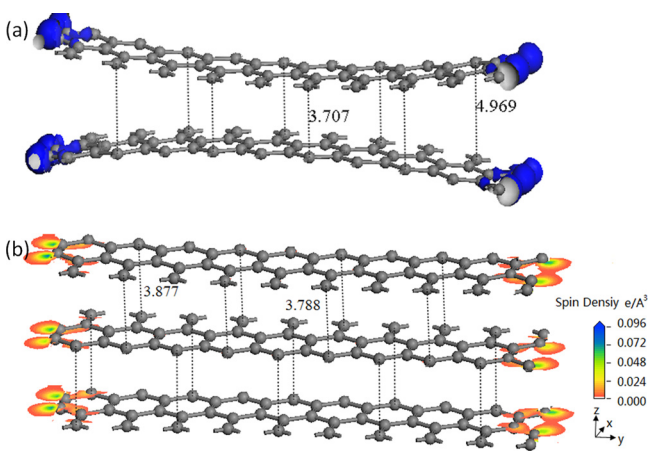

FIG. 4. (a) Large amount of excess electrons (e $= -3$) induces structural distortion and localized spin at edge of bilayer AGNR. The iso-surface of spin electron density is 0.021 e/Å^3. (b) Spin density distribution of trilayer AGNR induced by excess electrons (e $= -2$). Numbers between layers indicate the distances.

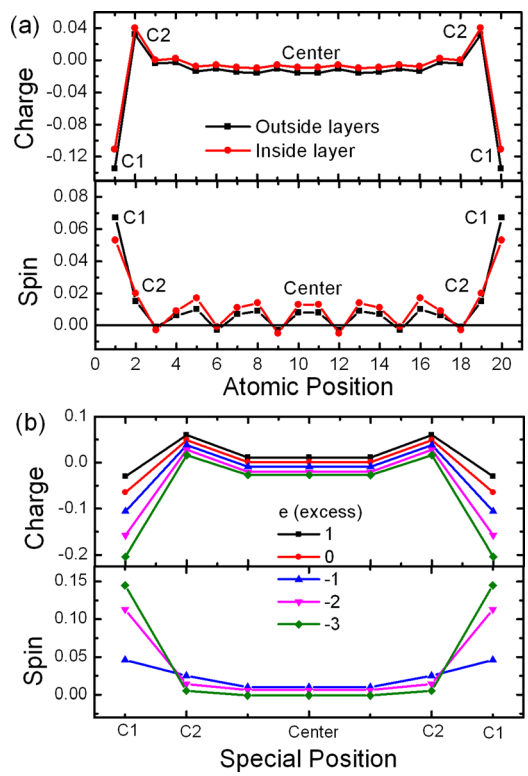

FIG. 5. (a) The profiles Mulliken of charge and spin along the ribbon width direction of trilayer AGNR for e(excess) $= -2$. Populations in two outside layers of AGNR are symmetric as plot by black squares while red circles represent those of inside layer. Negative charge sign means electron gain. (b)The value of Mulliken charge and spin at special sites (C1, C2, Center) on bilayer AGNR for different e(excess). Only non-zero spin distributions are plot.

C-C bonds at C2 site slightly expand to 0.1427 nm (by 0.5%) in outside layer.

Charge distribution shows that a large proportion (74%) of negative charges (sum of charges at C1 sites in a unit cell divided by *e*(excess)) is localized at C1 sites. The rest excess electrons are distributed quite uniformly among inside carbon atoms, except sites around C2. The atoms at C2 sites show a fluctuation of electron loss between C1 and center atoms. Spin result shows that a large proportion (69%) of net spin (sum of spin at C1 sites divided by total spin in a unit cell) is localized at C1 sites. The rest sites in the interior of AGNR show a few net spin. The similar profile was also obtained for monolayer AGNR (Figure S4[19]). The net spin localized at the edge mainly attributes to the p_z electrons, as identified by the shape of the density and also the orbital-resolved Mulliken analysis. Results verified that the excess charge captured by edge-quantum well induces ordered localized magnetism at armchair edge. Moreover, the outside layers show more significant edge-trapping effect than the inside layer of trilayer AGNR.

Figure 5(b) shows net charge and net spin distributions along the width direction at special sites (C1, C2, Center) of bilayer AGNR. Although *e*(excess) varies, charges are always transferred to C1 site due to the under-coordination induced edge-quantum well. Within proper amounts of *e*(excess), the spins are mainly generated at C1 sites. The same trends are also obtained for other thicknesses (Figures S5 and S6 (Ref. 19)). Above results again verified that excess charges are trapped by edge-quantum well and hence net spins are induced.

In summary, stable magnetism was proved to be generated at originally diamagnetic armchair edges under the condition of proper amount of excess electrons. The consistency between theoretical calculation and experiments clarified that (i) Graphene is stable with excess negative charges due to the under-coordination-induced edge-quantum well; (ii) Excess electrons can provide unpaired spin and induce relatively large magnetic moment, but too large amount of excess electrons will degenerate the spin, and thus, the generation of magnetism of excess electrons is quantity-dependent; and, (iii) Graphene is not stable with excess positive charges. Thus, in ECR experiment, edge-quantum well of multi-layer graphene nanoflakes can capture electrons from plasma beam in the growing process and induce a considerable magnetism. Considering only spin magnetic moment, DFT calculations result in large *M* values as 19.25, 6.78, and 5.45 emu/g for perfect monolayer, bilayer, and trilayer AGNRs, respectively, with 2 excess electrons per unit cell. According to calculation results, there is still plenty of room for enhancing *M* in experiments. Hence, the robust mechanism of magnetism in charged-graphene proposed herewith shed light on the development of graphene devices in its potentially magnetic applications.

[1]L. Brey and H. A. Fertig, Phys. Rev. B **73**, 235411 (2006).
[2]K. S. Novoselov, A. K. Geim, S. V. Morozov, D. Jiang, M. I. Katsnelson, I. V. Grigorieva, S. V. Dubonos, and A. A. Firsov, Nature **438**, 197–200 (2005).
[3]T. Enoki, Y. Kobayashi, and K. I. Fukui, Int. Rev. Phys. Chem. **26**, 609–645 (2007).
[4]C. Soldano, A. Mahmood, and E. Dujardin, Carbon **48**, 2127–2150 (2010).
[5]K. S. Novoselov, Z. Jiang, Y. Zhang, S. V. Morozov, H. L. Stormer, U. Zeitler, J. C. Maan, G. S. Boebinger, P. Kim, and A. K. Geim, Science **315**, 1379 (2007).
[6]C. L. Kane and E. J. Mele, Phys. Rev. Lett. **95**, 226801 (2005).
[7]M. Zeng, L. Shen, H. Su, C. Zhang, and Y. Feng, Appl. Phys. Lett. **98**, 092110–092113 (2011).
[8]H. Lee, Y.-W. Son, N. Park, S. Han, and J. Yu, Phys. Rev. B **72**, 174431 (2005).
[9]M. M. Ugeda, I. Brihuega, F. Guinea, and J. M. Goez-Rodriuez, Phys. Rev. Lett. **104**, 096804 (2010).
[10]K.-I. Sasaki and R. Saito, Prog. Theor. Phys. Suppl. **176**, 253–278 (2008).
[11]T. Enoki, S. Fujii, and K. Takai, Carbon **50**, 3141–3145 (2012).
[12]T. Wassmann, A. P. Seitsonen, A. M. Saitta, M. Lazzeri, and F. Mauri, J. Am. Chem. Soc. **132**, 3440–3451 (2010).
[13]X. Zhang, Y. Nie, W. Zheng, J.-l. Kuo, and C. Q. Sun, Carbon **49**, 3615–3621 (2011).
[14]M. Sepioni, R. R. Nair, S. Rablen, J. Narayanan, F. Tuna, R. Winpenny, A. K. Geim, and I. V. Grigorieva, Phys. Rev. Lett. **105**, 207205 (2010).
[15]Y. Kobayashi, K.-i. Fukui, T. Enoki, and K. Kusakabe, Phys. Rev. B **73**, 125415 (2006).
[16]T. Kawai, Y. Miyamoto, O. Sugino, and Y. Koga, Phys. Rev. B **62**, R16349–R16352 (2000).
[17]Y. H. Lee, S. G. Kim, and D. Tománek, Phys. Rev. Lett. **78**, 2393–2396 (1997).
[18]C. Wang and D. Diao, Appl. Phys. Lett. **102**, 052402 (2013).
[19]See supplementary material at http://dx.doi.org/10.1063/1.4891558 for the experimental method, spin density distribution of AGNRs, structural distortion, and the population along the ribbon width direction for different thicknesses.
[20]X. Zhang, J.-L. Kuo, M. Gu, P. Bai, and C. Q. Sun, Nanoscale **2**, 2160–2163 (2010).
[21]C. Q. Sun, Prog. Mater. Sci. **54**, 179–307 (2009).
[22]C. Coletti, C. Riedl, D. S. Lee, B. Krauss, L. Patthey, K. von Klitzing, J. H. Smet, and U. Starke, Phys. Rev. B **81**, 235401 (2010).
[23]Q. Jiang, L. H. Liang, and D. S. Zhao, J. Phys. Chem. B **105**, 6275–6277 (2001).
[24]T. Yi-Chou, H. Chia-Wei, Y. Jen-Shiang, L. Gene-Hsiang, W. Yu, and K. Ting-Shen, Angew. Chem., Int. Ed. **47**, 7250–7253 (2008).
[25]C. Q. Sun, H. L. Bai, B. K. Tay, S. Li, and E. Y. Jiang, J. Phys. Chem. B **107**, 7544–7546 (2003).
[26]K. Schouteden, E. Lijnen, D. A. Muzychenko, A. Ceulemans, L. F. Chibotaru, P. Lievens, and C. Van Haesendonck, Nanotechnology **20**, 395401 (2009).
[27]X. Fan, L. Liu, J. Lin, Z. Shen, and J.-L. Kuo, ACS Nano **3**, 3788–3794 (2009).
[28]B. Delley, J. Chem. Phys. **92**, 508–517 (1990).
[29]J. P. Perdew, K. Burke, and M. Ernzerhof, Phys. Rev. Lett. **77**, 3865 (1996).
[30]A. Tkatchenko and M. Scheffler, Phys. Rev. Lett. **102**, 073005 (2009).